Tectonophysics xxx (2014) xxx–xxx

Contents lists available at ScienceDirect

Tectonophysics

journal homepage: www.elsevier.com/locate/tecto

Significant rotations related to cover–substratum decoupling: Example of the Dôme de Barrôt (Southwestern Alps, France)

Lionel Sonnette [a,b,*], Fabien Humbert [c,d], Charles Aubourg [e], Jérôme Gattacceca [f], Jian-Cheng Lee [b], Jacques Angelier [a]

[a] UMR Géosciences Azur, CNRS-Université Nice Sophia-Antipolis, 250 av. Einstein, 06560 Valbonne, France
[b] Institute of Earth Sciences, Academia Sinica, 128 Academia Road, Section 2, Taipei 115, Taiwan
[c] Institut de Physique du Globe de Strasbourg, 1 rue Blessig, 67084 Strasbourg, France
[d] Department of Geology, University of Johannesburg, PO Box 524, Auckland Park, 2006 Johannesburg, South Africa
[e] LFCR, UMR 5150, CNRS, Université de Pau et des pays de l'Adour, TOTAL, BP 1155, 64013 Pau Cedex, France
[f] CNRS, Aix-Marseille Université, CEREGE UM34, 13545 Aix-en-Provence, France

ARTICLE INFO

Article history:
Received 4 October 2013
Received in revised form 31 March 2014
Accepted 6 April 2014
Available online xxxx

Keywords:
Cover–substratum strain decoupling
AMS
Paleomagnetism
Western Alps
Dôme de Barrôt

ABSTRACT

The Barrôt area presents an important contrast of deformation between a foliated, faulted and non-rotated Permian substratum and a folded and strongly rotated Meso-Cenozoic sedimentary cover. The Permian substratum and the sedimentary cover are separated by a décollement level of Triassic gypsum. While numerous studies have been done on the Dôme de Barrôt (i.e., the Permian substratum), we focused our work on the deformed Meso-Cenozoic sedimentary cover around the Dôme de Barrôt where we measured and analyzed both the magnetic susceptibility fabrics and the paleomagnetic directions. Our results highlight an arcuate pattern of the directions of shortening trajectories revealed by type II–III fabrics of anisotropy of magnetic susceptibility (which predates the folding) and a later syn- or post-folding anticlockwise rotation of large amplitude ($64 \pm 14°$) for the sedimentary cover. The arcuate pattern of the directions of shortening and the different rotations between the Permian substratum and the sedimentary cover can be partly explained after restoring the paleogeographic location of the sedimentary cover before the Oligocene Alpine compression event. We tend to interpret the remaining 30° anticlockwise rotation as a result of the high efficiency of the Triassic gypsum décollement surface, a nearby regional left-lateral shear zone (RDFZ), and a possible near-field gravitational sliding near the later exhumed Dôme de Barrôt.

1. Introduction

The propagation of décollement surfaces into fold-and-thrust belts often results in a significant decoupling of deformation patterns between shallower and deeper units (Costa and Vendeville, 2002; Dahlen et al., 1984; Malavieille, 2010). Such decoupling with differential shortening rates in fold-and-thrust belts with respect to the substratum rocks under a décollement is usually evoked for explaining the arcuate shape of the shallower units (Macedo and Marshak, 1999; Vidal-Royo et al., 2009). In the foreland of the Western Alps, the fold-and-thrust belts of Castellane and Nice in France are typical examples of arcuate fold-and-thrust belts (Fig. 1A). The main décollement surface is located in the Triassic gypsum layers (Graham, 1981), along which the Meso-Cenozoic cover overthrusted the underlying Permian substratum (Fig. 1C). These fold-and-thrust belts were first documented being of convex curvature in late 70s (Siddans, 1979). It was more explicitly interpreted as an inherited structure or a primary arc-shaped feature (Weil and Sussman, 2004), based on the evidence of no paleomagnetic rotation in the Permian substratum in the "Dôme de Barrôt", the Argentera (Bogdanoff and Schott, 1977) and the Estérel massifs (Zijderveld, 1975). Later on, although Aubourg and Chabert-Pelline (1999) observed a 40° anticlockwise rotation at level of the Digne nappe in the Neogene sediments, they did not question the primary arc-shaped nature because the rotations was interpreted to be controlled and bounded by the inherited structural pattern. Nevertheless such interpretations remained skewed by not taking into account (1) the strain decoupling between the substratum and the shallow cover, and (2) the structural pattern near the shear zone of the Rouaine–Daluis Fault Zone (RDFZ, Fig. 1B).

The Dôme de Barrôt is located in the inner part of the fold-and-thrust belt of Castellane, to the Southwest of the Argentera crystalline massif (Fig. 1A). To the southern edge of this Permian dome, the Meso-Cenozoic sedimentary cover presents a spectacular arcuate shape bounded farther to the West by the RDFZ. From West to East, the trend of the fold axes turn from NE–SW to E–W. This area provides a good opportunity to study a possible decoupling of deformation between the Paleozoic substratum and the Meso-Cenozoic cover through

* Corresponding author at: Institute of Earth Sciences, Academia Sinica, 128 Academia Road, Section 2, Taipei 115, Taiwan.
E-mail address: lsonnette@earth.sinica.edu.tw (L. Sonnette).

http://dx.doi.org/10.1016/j.tecto.2014.04.009
0040-1951/

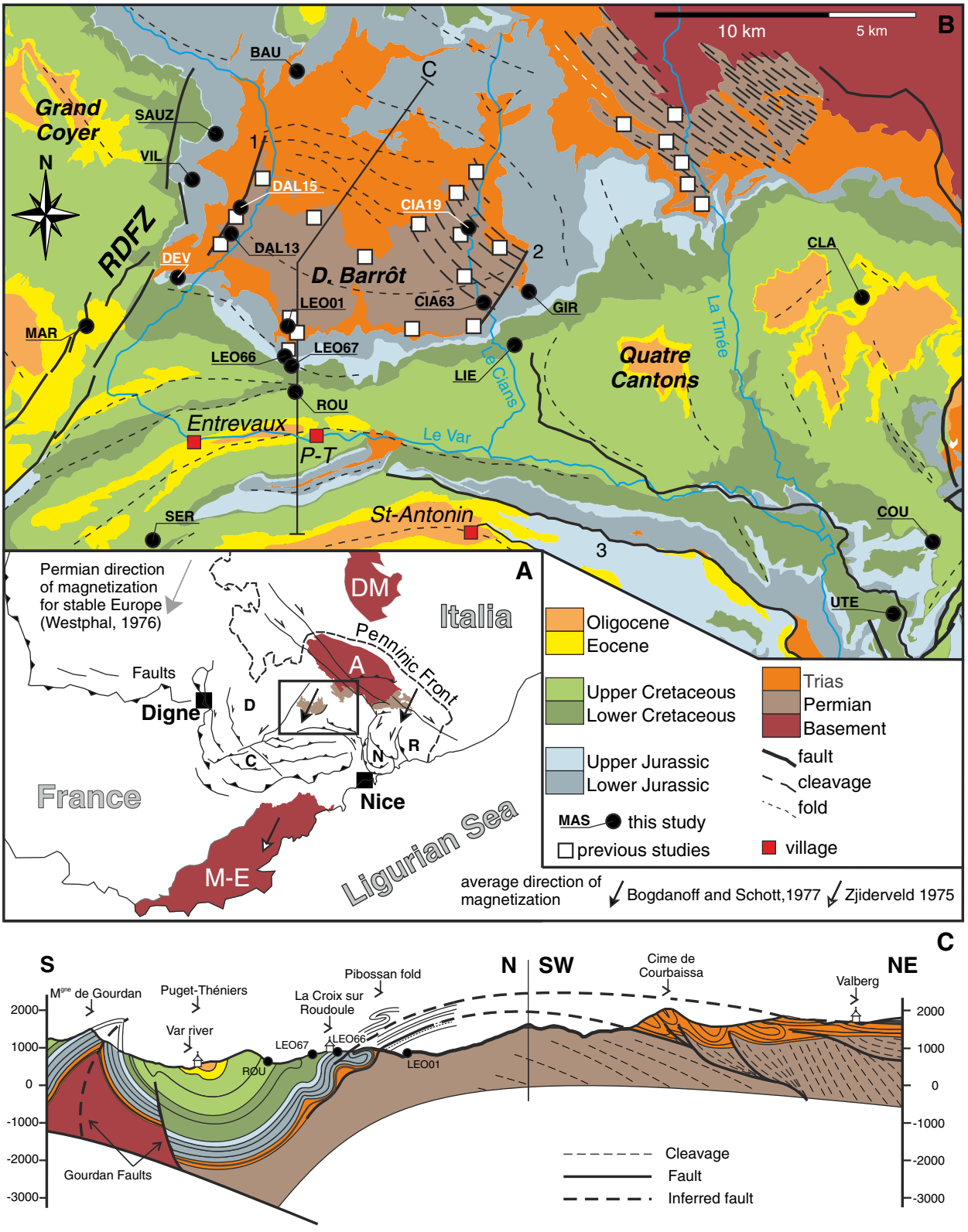

Fig. 1. (A) Geological context of the Dôme de Barrôt and location of the sampling sites in the study area. The black arrows represent the direction of magnetization for Permian layers (from Bogdanoff and Schott, 1977; Westphal, 1976; Zjiderveld, 1975). DM, A and M–E: Dora Maira, Argentera and Maures–Estérel crystalline basements; N: Nice salient; R: Roya salient; C: Castellane salient; D: Digne nappe. (B) Synthetic geological map of the studied area, modified from the geological maps of Puget–Théniers (Goguel et al., 1957) and Entrevaux (Campredon et al., 1980). The previous studies refer to the AMS and paleomagnetic works of Cogné and Perroud (1985), Graham (1978), Henry (1973), Kligfield et al. (1981), Siddans et al. (1984) and Van den Ende (1977). P–T: Puget–Théniers village. D. Barrôt: Dôme de Barrôt; 1: Daluis fault; 2: Girent fault; 3: Gourdan fault. (C) Geological cross-section through the Dôme de Barrôt.

the analysis of magnetic fabric and paleomagnetism. The decoupling that occurred between the Permo-Werfenian substratum and the Rhetian to Chattian sedimentary cover is probably due to the existence of a décollement of gypsum layers, the Muschelkalk and Keuper (Triassic) in age. For simplification of terminology, we use in this paper the terms Permian substratum or Paleozoic substratum and

Please cite this article as: Sonnette, L., et al., Significant rotations related to cover–substratum decoupling: Example of the Dôme de Barrôt (Southwestern Alps, France), Tectonophysics (2014), http://dx.doi.org/10.1016/j.tecto.2014.04.009

Meso-Cenozoic cover or sedimentary cover to refer to the units below and above the décollement respectively.

Analyses on Anisotropy of Magnetic Susceptibility (AMS) in non-metamorphic rocks allow determining the Layer Parallel Shortening (LPS) trends (Averbuch et al., 1992; Borradaile, 1988; Borradaile and Jackson, 2010), which generally formed in the early stage of rock deformation, usually prior to folding (Aubourg et al., 2004; Parés et al., 1999; Weil and Yonkee, 2009). On the other hand, paleomagnetic data are able to document about possible block horizontal rotations. AMS is thus an excellent marker of deformation and can test the reliability of paleomagnetic rotations. Studies of paleomagnetism have been broadly conducted for determining horizontal block rotations in many orogens worldwide (e.g., Carey, 1955; Weil and Sussman, 2004). This paper intends to present recent results of AMS and paleomagnetic rotation within and around the Permian substratum at Dôme de Barrôt, in order to compare with the arcuate fold-and-thrust belt of the Meso-Cenozoic cover. The results also allow us to discuss the possible complex mechanisms including décollement overthrusting, thrust-stack crustal thickening (Ford et al., 1999; Labaume et al., 2008), gravitional sliding (Graham, 1981) and blind thrusting (Ford et al., 1999; Laurent et al., 2000), on the finite deformation of the sedimentary cover.

2. Geological setting

The Permian substratum, which constitutes the Dôme de Barrôt (Fig. 1B), is composed of a thick series (<1 km) of continental deposit of red mudstones and slates issued from the erosion of the Variscan relief (Bourquin et al., 2011). It is unconformably overlain by Triassic quartzites and gypsum layers (Bordet, 1950; Vernet, 1958).

During the Alpine Tethys opening in Jurassic (deposition of Hettangian limestone to Oxfordian black shale), the Permian strata of Dôme de Barrôt were slightly exhumed and accompanied by N20–30° trending normal faulting on its western and eastern sides (Fig. 1B): the Daluis fault (Delpech, 1988) in the West and the Girent fault (Vernet, 1958) in the East. The South of the Dome is also bounded by a few large E–W and ESE–WNW trending normal faults, such as the Gourdan fault, delimiting the Dauphinois basin from the Provencal platform (Dardeau, 1988). After a tectonic inactive period during Malm (De Graciansky and Lemoine, 1988) concordant with the deposit of massive Tithonian limestone, the opening of the Alpine Tethys continued together with the formation of the Vocontian basin (Cotillon, 1971). During Early Cretaceous, from Berriasian to Aptian, several Jurassic normal faults were reactivated, in particular the Gourdan fault (Cotillon, 1971; Dardeau, 1988; De Graciansky and Lemoine, 1988). They bounded the calcareous platform from the Vocontian basin. Afterwards, the whole area was covered by late Albian to early Cenomanian calcareous sandstone and shale.

The late Cretaceous to Paleocene Pyreneo-Provence stage was marked by the transition from oceanic to continental subduction (e.g., Agard et al., 2009; Apps et al., 2004), which is presumably responsible for the uplifting of the Maures–Estérels and the Corsica massifs and the folding of the future Alpine foreland basin (Campredon, 1977). There is no evidence of deposits around the Dôme de Barrôt area during this period. Thereafter, during the Alpine continental collision initiated in the middle Eocene, a syn-orogenic transgression of continental deposition took place progressively westward of the Dome (Sztrákos and du Fornel, 2003). The deposit of Eocene syn-orogenic sediments was related to the southwestward advance of the Embrunais–Ubaye nappe (Labaume et al., 2008). The propagation of this nappe, suspected to extend southward to the Saint-Antonin syncline (Fig. 1B, Ford et al., 1999), provides evidence for a compressive stage lasted from late Priabonian (35 Ma) to Chattian (28.5 Ma) (e.g., Sztrákos and du Fornel, 2003). This event is responsible for: (1) a NE–SW trending deformation gradient under a predominant N40–50° shortening direction causing a NW–SE trending schistosity dipping to the northeast in the Permian red-beds in the Cians and Tinée valleys (Henry, 1973; Graham, 1978; Kligfield et al., 1981; Siddans et al., 1984, Fig. 1B and C) associated with anchizone metamorphism (tectonic burial around 4–8 km depth, Siddans, 1980); (2) a reactivation of Permian and Triassic inherited faults (Delteil et al., 2003); and (3) a tectonic burial of the grès d'Annot formation at depth over 4 km (Labaume et al., 2008) following the northern burial of the Argentera crystalline basement. As the Permian substratum is stuck to the Argentera crystalline basement, the burial of the Dôme de Barrôt (Siddans, 1980) was presumably synchronous with the underthrusting of the Argentera massif, dated around 23–34 Ma (Sanchez et al., 2011b).

From the Chattian to Present day, the Argentera Massif continued to be exhumed, accompanied by transcurrent motions (e.g., Sanchez et al., 2011a). Doming with E–W anticlinal folding and normal faulting (Schuiling, 1956; Vernet, 1958), and the southeast and southwest verging folding provide several pieces of evidence for the uplifting of the Dôme de Barrôt, certainly coeval with the exhumation of the Argentera Massif. This latest period corresponds also to the development of E–W trending folds and southward verging thrusts of both the Castellane (Laurent et al., 2000) and the Nice fold-and-thrust belts (Giannerini et al., 2011; Ritz, 1992).

The sedimentary cover shows hectometric to pluri-kilometric folds in the studied area (Fig. 1B and C). In the north, the Middle Triassic strata (Muschelkalk) form a series of tightened, inclined and recumbent folds with WNW–ESE trending fold axis (Bordet, 1950, Fig. 1C). However, the Upper Jurassic and Cretaceous formations are not affected by such folding. In the south, the whole cover, from Muschelkalk to Turonian, is affected by overturned folding verging both to the south as the Pibossan fold (Bordet, 1950; Vernet, 1958, Fig. 1C) and to the SW. These folds are similar to the décollement folds described in the Upper Var Valley to the north of Dome (Gubler et al., 1967). At the location of the gypsum diapir of Puget–Thénier, the trend of fold axis changes from WNW–ESE trending at East to NE–SW at West (Fig. 1B). This ductile pattern, that we call the 'fold of Entrevaux', was previously interpreted either to have been glided over the substratum (Graham, 1981) due to the exhumation of Argentera and Barrôt massifs during the Miocene or in response to the tectonic burial by underthrusting during the Oligocene (Ford et al., 1999; Laurent et al., 2000). In both cases, the Triassic gypsum, which is of a nature of relatively low mechanical friction, played an important role on acting as the décollement surface.

3. Sampling and methods

We sampled at 19 sites (Fig. 1B and Table 1) with a total of 526 oriented standard specimens for magnetic analyses within and around the Dôme de Barrôt for both the Permian substratum and the Meso-Cenozoic cover. The core-samples were collected by using an electric drill cooled by water and supplied by a generator. The orientation of the cores was measured in situ by a compass and an inclinometer. Five sites (DAL13, DAL15, CIA19, CIA63 and LEO01) are located in the Permian slate/mudstone substratum (Figs. 1 and 2A). Other 14 sites were sampled in the Meso-Cenozoic sedimentary cover at variable distance to the Dôme de Barrôt. We sampled in the different rock formations, including the Callovo-Oxfordian black shale (BAU, GIR, DEV, VIL, SAUZ and LEO66; Fig. 2A), the Neocomian marly limestone (LEO67, LIE, UTE and COU; Fig. 2A), the Cenomanian calcareous shale (ROU and SER; Fig. 2A), and the Priabonian blue shale (MAR and CLA; Fig. 2A). Only the three Jurassic sites BAU, VIL and SAUZ reveal an E–W trending schistosity dipping slightly to the north (Fig. 1B); the other sites show good preservation of original sedimentary bedding without schistosity.

AMS was measured using a spinner kappabridge KLY-3 (Agico Ltd.) at the Geosciences Environment Cergy laboratory of the University of Cergy-Pontoise (France) for sites BAU, GIR and CLA, and at the CEREGE (Aix-en-Provence, France) for all other sites. The AMS results were computed from Jelinek methods (Jelínek, 1978). The measurements of the remanent magnetization were carried out using a 2G SQUID

Please cite this article as: Sonnette, L., et al., Significant rotations related to cover–substratum decoupling: Example of the Dôme de Barrôt (Southwestern Alps, France), Tectonophysics (2014), http://dx.doi.org/10.1016/j.tecto.2014.04.009

Table 1
Structural, paleomagnetic and magnetic results for sampled sites. S_0 corresponds to the bedding expressed by the azimuth of the dip direction and dip in degrees. N = number of samples measured; K_m = bulk susceptibility; P_j = corrected degree of anisotropy; T = shape factor; K_{1-3} = maximum and minimum susceptibility in situ and after untilting of the bedding respectively; N/N_0 = number of interpreted samples over the number of measured samples; D = declination; I = inclination; *Type* = type of magnetic fabric; α_{95} = 95% Fisher confidence error (Fisher, 1953); k = dispersion.

General				Anisotropy of magnetic susceptibility								Remanent magnetization							
Site	Lat (°)	Lon (°)	S_0 (°)	N	$K_m \times 10^{-6}$	P_j	T	$K_{1\ \text{in situ}}$ (D/I in °)	$K_{3\ \text{in situ}}$ (D/I in °)	$K_{1\ \text{tecto}}$ (D/I in °)	$K_{3\ \text{tecto}}$ (D/I in °)	Type	Component	N/N_0	$D_{\text{in situ}}$ (°)	$I_{\text{in situ}}$ (°)	D_{tecto} (°)	I_{tecto} (°)	α_{95} (°)	k
MAR	44.000	6.753	344/23	12	78.9 ± 8.2	1.029 ± 0.004	−0.53 ± 0.16	86/5	182/52	88/26	201/38	III	Mar-B	11/15	27	41.7	17.8	23.5	10.1	21.3
													Mar-A	11/15	109.3	−59.2	129.5	−42.5	5.9	61.3
CLA	44.016	7.214	212/12	19	98.0 ± 28.1	1.025 ± 0.016	0.37 ± 0.27	180/13	80/36	171/2	93/47	II								
SER	43.907	6.792	319/71	10	73.1 ± 18.5	1.010 ± 0.007	0.00 ± 0.44	230/7	138/19	235/1	43/89	II	Ser-B	10/12	6.3	72.7	331.7	6.9	8.8	31.4
													Ser-A	10/12	148.4	64.3	313.3	44.2	8.0	37.5
ROU	43.975	6.879	173/59	14	27.2 ± 1.1	1.012 ± 0.009	0.07 ± 0.45	78/3	347/25	83/6	310/82	II	Rou	13/26	332.8	30.3	260	72.6	12.5	12.0
LIE	43.991	7.004	36/17	11	125.2 ± 3.9	1.038 ± 0.008	0.47 ± 0.13	73/14	332/37	256/6	21/79	II	Lie	9/9						
LEO67	43.985	6.872	195/27	15	60.9 ± 4.5	1.036 ± 0.003	−0.04 ± 0.12	273/7	20/66	271/1	158/87	II	Leo67-B	13/20	47.4	79.2	176.8	71.3	11.8	13.4
													Leo67-A	16/20	305.7	47.3	274.3	49.8	9.4	16.4
COU	43.879	7.233	136/56	9	4780 ± 349	1.027 ± 0.008	0.60 ± 0.12	124/34	302/56	306/12	167/74	II	Cou	0/7						
UTE	43.993	6.760	075/27	11	212.4 ± 35.7	1.018 ± 0.003	0.49 ± 0.27	156/2	251/63	336/2	160/88	I	Ute	5/8	5.4	58.6	33.4	42.7	14.9	27.2
DEV	44.023	6.808	215/51	13	825.5 ± 158.5	1.024 ± 0.008	0.03 ± 0.31	309/4	42/38	304/6	121/84	II	Dev	15/17	6.5	72.5	229	53.6	9.0	18.8
VIL	44.056	6.830	335/23	12	165.3 ± 4.7	1.048 ± 0.003	0.76 ± 0.07	275/16	116/73	279/2	14/73	II	Vil	20/23	356.5	68.6	345.6	43.5	2.8	134.3
SAUZ	44.088	6.838	354/33	12	238.2 ± 7.3	1.076 ± 0.006	0.71 ± 0.07	253/6	352/55	258/15	354/24	IV	Sauz-B	14/14	349.5	76.4	352.6	43.4	8.3	24.0
													Sauz-A	4/14	161.5	−6.9	160.2	25.3	11.9	60.8
LEO66	43.988	6.871	191/52	8	162.4 ± 37.1	1.042 ± 0.021	0.32 ± 0.16	262/11	6/51	81/8	206/77	II	Leo66	5/9	332.5	24.3	292.4	54.6	12.6	37.8
BAU	44.135	6.910	180/05	25	233.6 ± 21.2	1.017 ± 0.012	0.11 ± 0.25	321/1	52/41	321/6	56/43	II								
GIR	44.010	7.015	170/52	28	683.0 ± 70.2	1.014 ± 0.005	0.05 ± 0.37	215/28	67/58	30/12	129/28	II								
CIA19	44.055	6.979	20/11	10	170.1 ± 17.0	1.035 ± 0.005	−0.41 ± 0.24	128/2	222/67	127/5	239/77	III								
CIA63	44.006	6.992	143/26	11	189.5 ± 19.8	1.031 ± 0.003	0.09 ± 0.21	109/2	213/84	287/20	156/61	III								
DAL13	44.047	6.843	279/15	13	290.8 ± 22.6	1.058 ± 0.009	0.66 ± 0.23	317/15	101/72	315/3	112/87	II								
DAL15	44.060	6.853	19/34	7	252.6 ± 30.3	1.049 ± 0.014	0.54 ± 0.15	299/8	161/79	121/0	30/70	II								
LEO01	44.004	6.874	216/28	15	156.4 ± 35.3	1.021 ± 0.018	0.45 ± 0.34	267/27	58/60	264/5	137/81	I								

magnetometer at the CEREGE. A pilot paleomagnetic analysis was performed on two samples for each site: one sample for thermal demagnetization and the other for alternative field (AF) demagnetization. In the course of thermal demagnetization, we also monitored the low-field magnetic susceptibility to detect possible changes in magnetic mineralogy. The data analysis of the demagnetization of the natural remanent magnetization (NRM) was conducted using the Paleomac software (Cogné, 2003). Amount of horizontal block rotation and inclination difference were calculated as the declination and inclination angular differences compared to a given virtual geomagnetic pole of reference from Torsvik et al. (2008). The uncertainties of rotation and inclination difference have been estimated by combining the uncertainties of both the measured magnetization and the virtual geomagnetic pole of reference using the correction proposed by Demarest (1983).

4. Results of rock magnetism

4.1. General characteristics

The majority of the samples, as well as from the Permian substratum and the Meso-Cenozoic cover, presents weak mean susceptibility K_m ($15 < K_m < 300$ μSI), and weak NRM intensity values (between 40 and 700 μA/m), revealing a low concentration of ferromagnetic minerals (Table 1). Nevertheless, some samples from the Jurassic and Cretaceous black shales (sites DEV, GIR and COU) are characterized by a stronger mean susceptibility of $600 < K_m < 1000$ μSI and an intensity of NRM about 7000 μA/m, exhibiting a higher ferromagnetic contribution.

For identifying the major magnetic minerals in different strata, we performed a thermal demagnetization of composite isothermal remanent magnetization (IRM) adopting the Lowrie (1990) on one sample for each rock formation. We are able to distinguish three components of coercivities H_c: the soft ($H_c < 0.1$ T), the medium ($0.1 < H_c < 0.5$ T) and the hard ($0.5 < H_c < 1$ T) components (Fig. 2C). The general pattern shows a few slight breaks of slope (2 or 3 on each graph of Fig. 2C), highlighting existence of several magnetic minerals. Especially the dominance of soft coercive component exhibits a maximum unblocking temperature near 600 °C in most of the samples from the sedimentary cover, except for the Callovo-Oxfordian black shale with a much lower unblocking temperature near 400 °C. This feature is consistent with the presence of magnetically soft magnetite (Curie point around 580 °C) as the main magnetic contributor for the samples in the sedimentary cover, except for site DEV where the iron sulfides are suspected to be the dominant magnetic minerals (Curie point around 330 °C). By contrast, thermal and AF demagnetization of the Permian samples reveals a high blocking temperature (over 650 °C) and a strong coercivity (over 100 mT), both characteristics of hematite.

4.2. AMS fabric

The directional results of AMS analyses, including strain type, magnetic foliation (or lineation) and shortening direction as well as their relation with bedding orientation, are presented in Fig. 3. The AMS defines a symmetric second-rank tensor which corresponds to an ellipsoid defined by three eigenvalues and associated axes, K_1, K_2 and K_3, respectively the maximum, intermediate and minimum susceptibility. The maximum axis K_1 defines the magnetic lineation and the minimum axis, K_3, corresponds to the pole of the magnetic foliation. In weakly deformed sedimentary rocks, several studies pointed out that the magnetic foliation (K_1–K_2 plane) is mainly a relic of the diagenetic compaction. In moderate to strongly deformed rocks, the magnetic lineation is mostly perpendicular to the LPS (Layer Parallel Shortening) direction (Aubourg et al., 2004; Averbuch et al., 1992; Borradaile and Henry, 1997; Weil and Yonkee, 2009). There are commonly four basic types of evolution of AMS fabrics facing increasing LPS in such kind of rocks (Averbuch et al., 1992; Aubourg et al., 2004; Robion et al., 2007, Fig. 3). The type I is characterized by a magnetic foliation parallel to

Please cite this article as: Sonnette, L., et al., Significant rotations related to cover–substratum decoupling: Example of the Dôme de Barrôt (Southwestern Alps, France), Tectonophysics (2014), http://dx.doi.org/10.1016/j.tecto.2014.04.009

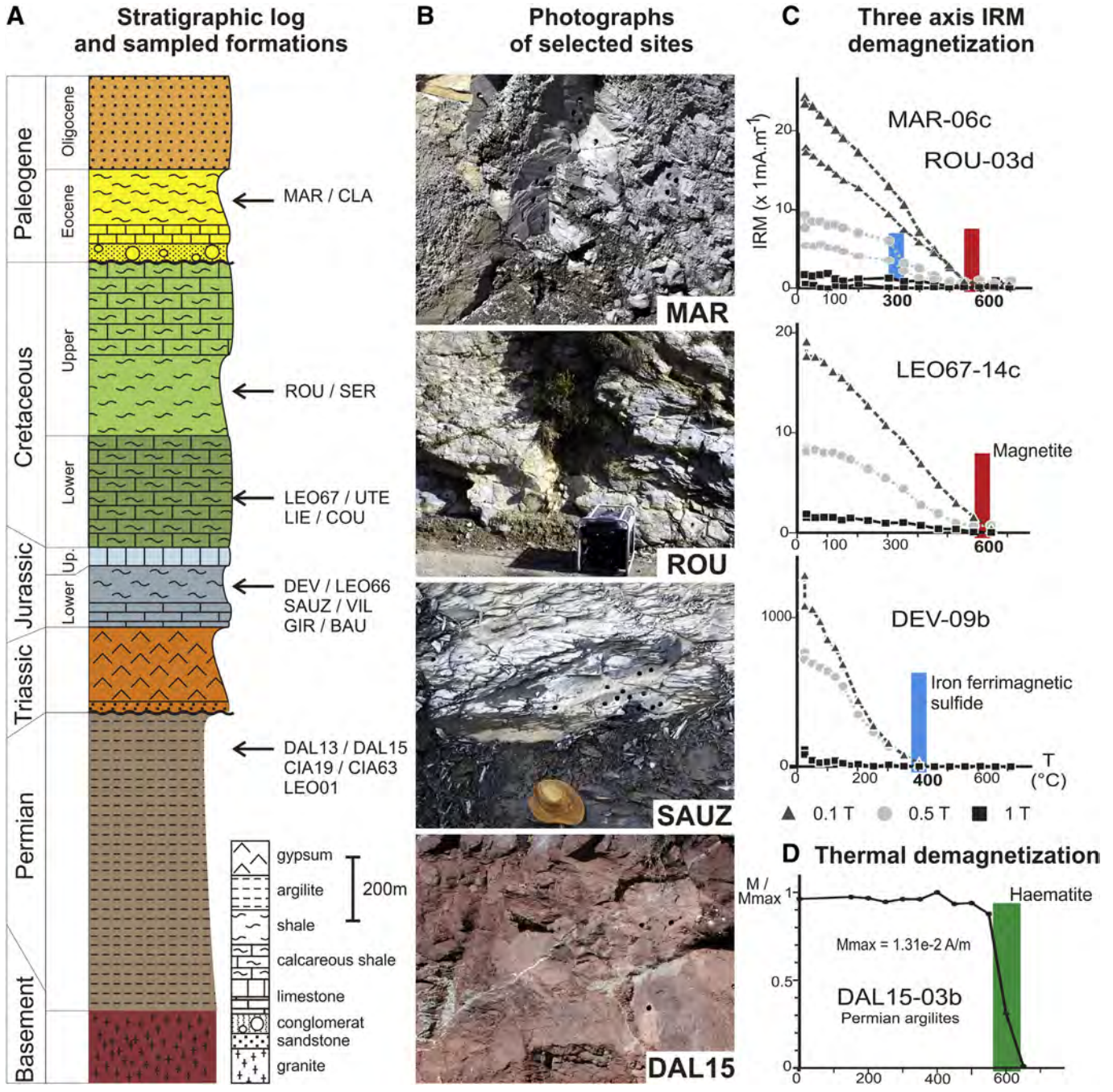

Fig. 2. (A) Schematic stratigraphic log of the studied area and related sampled sites. (B) Photographs of the sampled sites MAR, ROU, SAUZ and DAL15. (C) Stepwise thermal demagnetization curves along three isothermal remanent magnetization (IRM) components of some samples for the different layers sampled (Priabonien blue shales: MAR-06c; Cenomanian calcareous shales: ROU-03d; Neocomian marly limestones: LEO67-14c; Callovo-Oxfordian black shales: Dev09b). The main magnetic carriers are magnetite and iron ferrimagnetic sulfides. (D) Stepwise thermal demagnetization curve of the NRM for a Permian specimen, the magnetization shows high blocking temperature characteristics for hematite.

the bedding (i.e., K_3 is perpendicular to the bedding) and an absence of predominant magnetic lineation (a widespread of K_1). In response to a progressive increase of the intensity of the deformation, a predominant magnetic lineation first appears with a magnetic foliation being subparallel to the bedding (type II), then the magnetic foliation disappears coeval with a progressive rotation of K_3 axis toward the shortening direction (type III), and finally the magnetic foliation appears again usually at high angle to the bedding (type IV).

Sixteen of nineteen sites exhibit magnetic fabric of types II and III (Fig. 3 and Table 1). Only two sites, from the substratum (LEO01) and the cover (UTE), are characterized by fabric of type I; and finally, one site, SAUZ of the cover, presents a fabric of type IV. All the distinguished magnetic lineations (i.e., K_1 axes) are horizontal or sub-horizontal before any bedding correction. All our Permian sites (DAL13, DAL15, CIA18 and CIA63) present a well-defined NW–SE trending magnetic lineation (i.e., NE–SW trending LPS), that is consistent with most of the sites of the previous studies for the Dôme de Barrôt and the Upper Tinée Valley (Graham, 1978; Henry, 1973; Kligfield et al., 1981; Siddans et al., 1984). This NE–SW trending LPS also was found at the Meso-Cenozoic cover sites located in the north (site BAU), and in the east (sites COU and CLA) of the Dôme de Barrôt. Whereas the sites located in the west (sites SAUZ and VIL) and south (sites LEO66, LEO67, ROU, MAR and LIE) of the Dome exhibit E–W trending magnetic lineation (i.e., N–S trending LPS) as well as the sites from Henry (1973) for the

Please cite this article as: Sonnette, L., et al., Significant rotations related to cover–substratum decoupling: Example of the Dôme de Barrôt (Southwestern Alps, France), Tectonophysics (2014), http://dx.doi.org/10.1016/j.tecto.2014.04.009

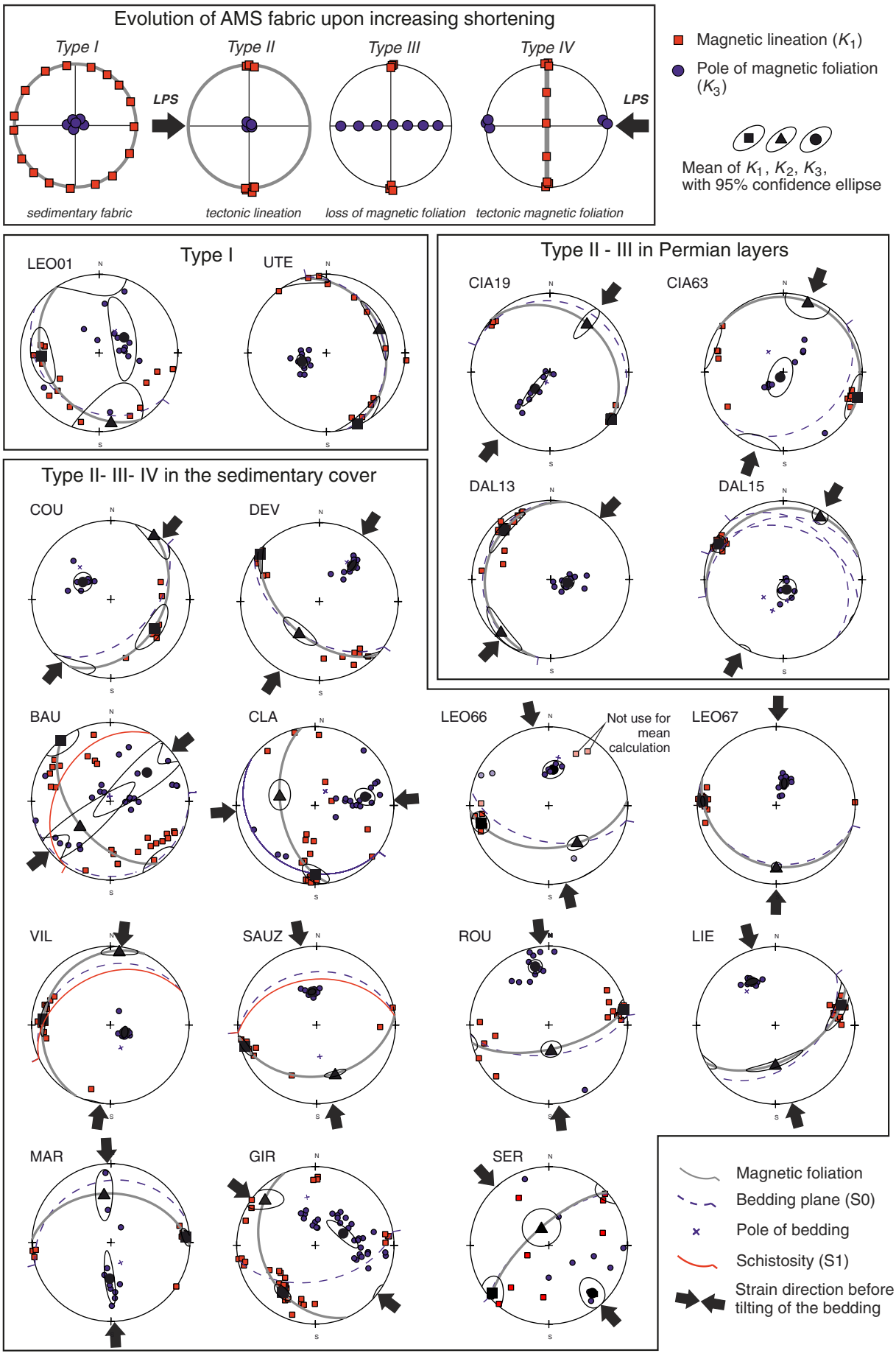

Please cite this article as: Sonnette, L., et al., Significant rotations related to cover–substratum decoupling: Example of the Dôme de Barrôt (Southwestern Alps, France), Tectonophysics (2014), http://dx.doi.org/10.1016/j.tecto.2014.04.009

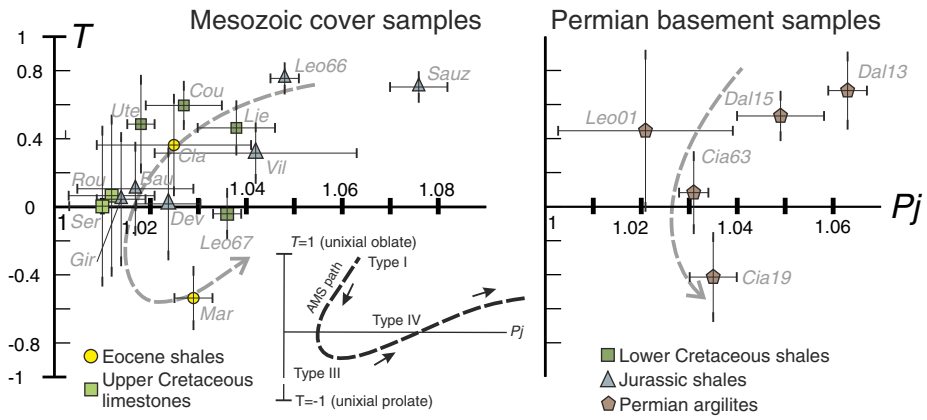

Fig. 4. Anisotropy shape parameter T versus corrected anisotropy degree P_j for Mesozoic cover (left) and Permian samples (right). In the synthetic T/P_j diagram (lower-middle), the black dashed line shows the general trend of the AMS ellipsoid shape during coaxial deformation. The gray dashed lines represent this trend both for Meso-Cenozoic cover and Permian substratum samples.
Modified from Borradaile and Henry (1997).

southern part of the Permian Dome. However, two sites (SER and GIR) present a NE–SW trending magnetic lineation direction (NW–SE LPS). In general, the different trends of magnetic lineation are spatially well organized in a consistent way. Concerning the chronological relation between the formation of the AMS fabrics and tectonic folding/tilting, it still remains difficult to tell after conducting the fold/tilt tests. For instance, we obtained a mean direction of magnetic lineation of N36 ± 10°/N36 ± 10°, before and after bedding correction, respectively, for the group with NE-direction AMS (sites COU, DEV, BAU) and a mean direction of N179 ± 12°/N176 ± 13°, before and after bedding correction, respectively, for the group with NS-direction AMS (sites LEO66, LEO67, VIL, ROU, LIE, MAR).

Additional information on AMS can be obtained from the analysis of the shape of the anisotropy ellipsoid characterized by the shape factor T and the corrected degree of anisotropy P_j introduced by Jelinek (1981). We plotted our results of T with respect to P_j for each site in Fig. 4. The AMS path drawn in the synthetic diagram of lower inset of Fig. 4 is an empirical strain path proposed by several authors (Aubourg et al., 2004; Borradaile and Henry, 1997; Parés, 2004; Robion et al., 2007) using corrugation of platy particles as an indication of magnetic fabric acquisition. Eleven out of nineteen sites reveal an oblate shape of ellipsoid ($T > 0.2$); six sites (SER, ROU, GIR, BAU, DEV and LEO67) show a triaxial shape ($-0.2 < T < 0.2$); and only 2 sites (MAR and CIA19) have a prolate shape ($T < -0.4$). Considering the Permian clastic sites, the results are consistent with a NE trending increase of the deformation as previously mentioned by Kligfield et al. (1981) and Siddans et al. (1984). Fabrics evolve from type I and type II (in the Daluis valley and in the southern part of the Dome) to type III fabric (in the Cians valley) (see locations in Figs. 1 and 3). On the contrary, the data from the Meso-Cenozoic cover are more scattered, probably due to significant lithological variations from carbonates to clayey rocks (Fig. 4 and Table 1). Even after facies distinction, no significant correlation of P_j, T and K_m parameters can be proposed with respect to the fabric type and their geographical locations. In the northwest, the site SAUZ, where schistosity has developed, show well defined magnetic fabric of type IV. We anticipate that the site SAUZ represents the more mature (stronger) deformation near the right end of the AMS path. However, it needs further investigations with more sites with obvious schistosity. On the other hand, one can observe a geographical correlation of triaxial fabrics ($-0.3 < T < 0.3$ and $P_j < 1.035$) in the sedimentary cover near the Paleozoic dome (sites BAU, DEV, GIR, LEO67), whereas oblate fabrics ($T > 0.3$ and $P_j > 1.035$) correspond to the furthest sites (LEO66, VIL, SAUZ and LIE).

4.3. Paleomagnetism

The remanent magnetization was measured exclusively on sites from the Meso-Cenozoic cover by performing either AF (from 0 to 100 mT in 20 steps in average) or thermal (until 300 °C with an average of 5 steps) then AF (until 100 mT in 10–16 steps) demagnetization, according to the pilot demagnetization profiles. We have just conducted a few demagnetizations on the Permian formations in order to confirm the presence of hematite (Fig. 2D) as they have already been the subject of numerous paleomagnetic studies (Bogdanoff and Schott, 1977; Cogné and Perroud, 1985; Henry, 1973; Kruiver et al., 2000; Van den Ende, 1977). In this Permian substratum unit, a primary reverse magnetization (declination of 210 ± 15°, inclination of −25 ± 10°) was characterized. This direction of magnetization is concordant with that of Permian time for Eurasia (Bogdanoff and Schott, 1977; Westphal, 1976) and no explicit rotation is thus highlighted. Although the Alpine orogeny was proposed for the magnetization due to the parallelism of the magnetization with the NE–SW Oligocene direction of compression (Henry, 1973), fold tests (i.e., bedding correction tests) indicated that the magnetization was recorded before folding (Cogné and Perroud, 1985) and microprobe analyses highlighted that the magnetization was brought by titanium bearing hematite which supports a detrital and volcanic origin (Kruiver et al., 2000).

Paleomagnetism measurements were conducted on ten sites (Fig. 5A). Most of the sites provide significant paleomagnetic components (Table 1), which allow a principal component analysis. The only exceptions are the sites COU and LIE where samples present unstable magnetizations for which the principal component analysis is not relevant. Two behaviors can be observed with (1) one component and (2) two components of magnetization. Four sites (LEO66, LEO67, SAUZ and MAR) present two components of magnetization that we call A-component and B-component. The B-component has generally a low coercivity and a low unblocking temperature (2–20 mT and 25–300 °C). The A-component has higher coercivity, higher unblocking temperature and crosses the origin of demagnetization plot at the end of the demagnetization process (Fig. 5A). The four other sites (VIL, DEV, UTE and ROU) show only on component with the B-component type magnetic features.

Fig. 3. AMS results in the studied area. All results are presented in the in situ orientation before any bedding correction. The diagrams on the top represents the conceptual model of the evolution of an AMS fabric upon increasing shortening.
Modified from Averbuch et al. (1992) and Robion et al. (2007).

Please cite this article as: Sonnette, L., et al., Significant rotations related to cover–substratum decoupling: Example of the Dôme de Barrôt (Southwestern Alps, France), Tectonophysics (2014), http://dx.doi.org/10.1016/j.tecto.2014.04.009

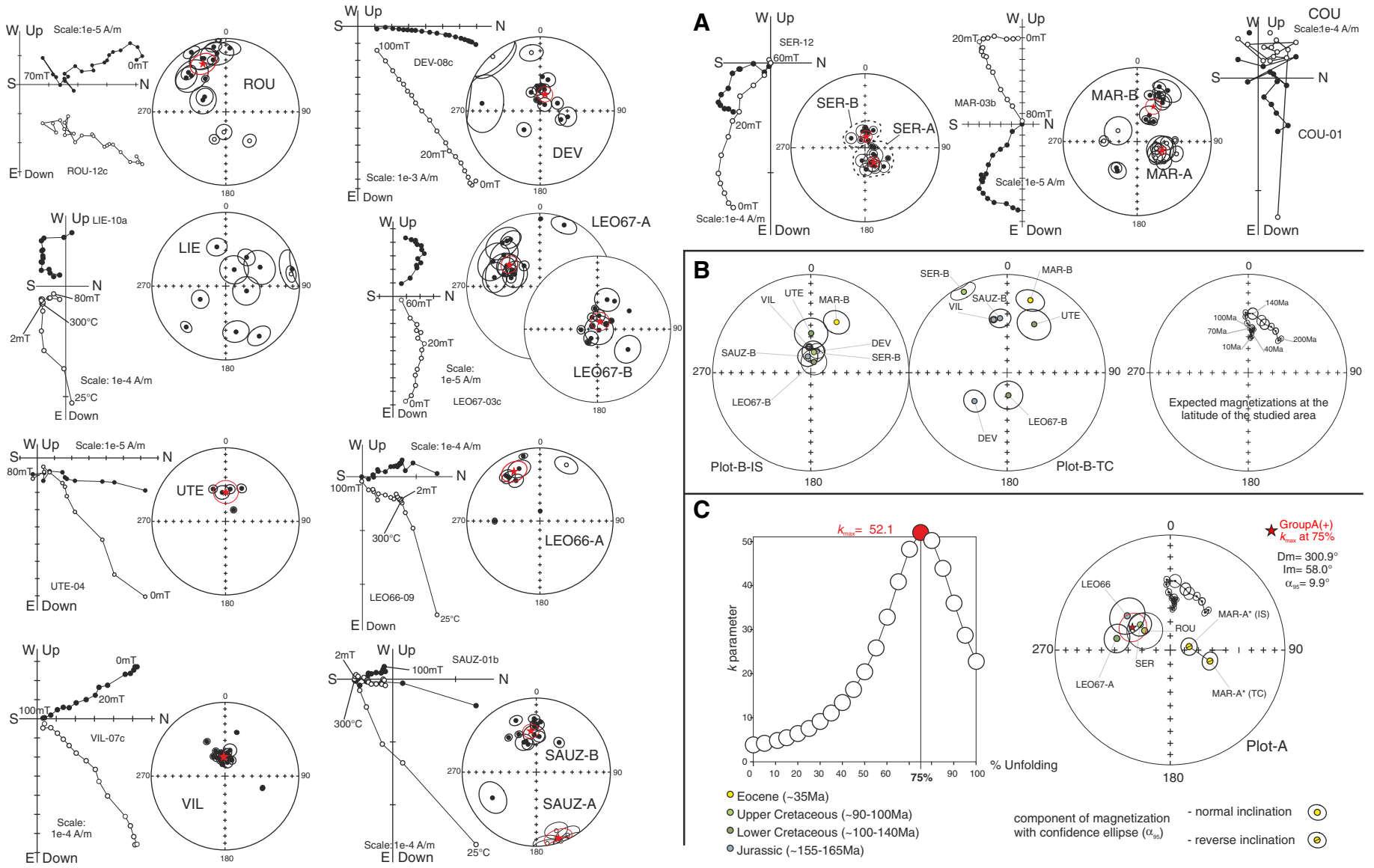

Fig. 5. Results of the paleomagnetic analysis. (A) Typical examples of orthogonal projection plots of stepwise demagnetization data for one specimen per site. The stereographic projections show all determined remanent magnetic components for the corresponding sites. All the results are presented in in situ orientations. Open (closed) symbols represent projections onto the vertical (horizontal) plane in orthogonal plots and reverse (normal) polarity in stereographic plots. (B) In situ (left stereo) and tectonic corrected (TC; middle stereo) results of the B-component magnetizations. The right stereo show the expected magnetizations at the latitude of the Dôme de Barrôt calculated from the apparent polar wander path for Europe from 200 Ma to 10 Ma (Torsvik et al., 2008). (C) Fold test for A(+)-group and folding trajectory of MAR-A after correction of MAR-B component. The left plot presents the evolution of the dispersion parameter k during an homogeneous backtilting of the stratification for the sites included in the A(+)-group. The stereo shows the configuration of magnetizations of the A(+)-group at 75% of unfolding. The folding trajectory of the component MAR-A* (=MAR-A corrected from MAR-B, see Table 2) from in situ position (IS) to after bedding correction position (TC) is also presented. The red star corresponds to the mean magnetic direction for the A(+)-group at 75% of unfolding. Dm = declination, Im = inclination and α_{95} = corrected Fisher confidence error (Demarest, 1983).

Please cite this article as: Sonnette, L., et al., Significant rotations related to cover–substratum decoupling: Example of the Dôme de Barrôt (Southwestern Alps, France), Tectonophysics (2014), http://dx.doi.org/10.1016/j.tecto.2014.04.009

The results for the samples with the A- and B-components are plotted together in stereographic projection (Fig. 5B and C). A tilt test of bedding correction (McFadden and Jones, 1981) has been carried out. The B-components are close in declination to the present day magnetic field. Note that the Callovo-Oxfordian black shale has a strong inclination (sites VIL, DEV, SAUZ and LEO67-B, mean vector: declination = 4.1°, inclination = 74.5°, α_{95} = 7.5° and dispersion k = 149.3). In contrast, the Priabonian blue shale has rather a low inclination and a declination suggesting a potential clockwise rotation. The tilt test shows unambiguously a large scattering of B-components (Fig. 5B), which is therefore interpreted to be post-folding in chronological order between magnetization and folding (or tilting). As a result, the magnetization of the B-component is possibly a viscous remagnetization acquired during the last million years although relatively high unblocking temperature (~300 °C) could suggest another cause of remagnetization.

In their original in situ orientations, the A-components (sites SER-A, LEO66-A, LEO67-A, MAR-A, ROU) have distinct directions and are far away from the present day magnetic field (Fig. 5C). Among the A-components sites, we also define the A(+)-group, composed by the sites ROU, LEO66, LEO67 and SER, which are located in both limbs of the fold of Entrevaux and show almost exclusive normal polarities (50 of 55 specimens, Figs. 1C and 5A). By contrast, the A-component of site MAR-A has a reverse polarity. The A-components of the A(+)-group show a best clustering at 75% of unfolding. At unfolding stage, the mean inclination is consistent with the expected inclination for the Meso-Cenozoic period (Middle Jurassic to Miocene; Fig. 5C). As a consequence, the magnetization of the A(+)-group can thus be interpreted as syn-tilting remagnetization. The few reverse polarity magnetizations of sites ROU and LEO66 (Fig. 5A) of other A-components are too scattered and not representative of the average trend to allow a pertinent reversal test and for invalidating a syn-folding remagnetization. At 75% of unfolding, the mean magnetization is oriented N301° with inclination of 58°. The component MAR-A, after a first correction of both rotation and inclination difference according to the data obtained for MAR-B (see MAR-A*, Fig. 5C and Table 2), has a declination all along the tilting path ranges from 79° to 106°, suggesting an anticlockwise rotation of 70–110° (Fig. 5C).

5. Discussion

The study of magnetic fabrics and paleomagnetic directions in the Meso-Cenozoic cover around the Paleozoic Dôme de Barrôt brings specific results. On the one hand, the AMS data highlight a similar discrepancy in the direction of magnetic lineation between a NW–SE trend in the northeastern side to E–W trends in the southern side for both the Permian substratum and the overlying Meso-Cenozoic cover. On the other hand, the paleomagnetic data from the cover in the southwest of the Dome reveal an important anticlockwise horizontal rotation of 64° whereas the Permian substratum recorded no rotation. Hereafter, we discuss the geological information and its relationships with our AMS fabrics (in a first part), our paleo remanent directions (in a second part) and the interpreted rotations (in a third part). Finally, we propose a synthesis of the geological history of the Dôme de Barrôt area with the major deformation processes involved.

5.1. AMS a marker of the Alpine directions of shortening

Our results of AMS fabrics denote a dominance of type II and type III fabrics with oblate and triaxial shapes and horizontal magnetic lineations in the in situ orientation. In weakly deformed non-metamorphic sedimentary rocks, the magnetic foliation remains generally parallel to the bedding while the magnetic lineation can align to either sedimentary features (current of flow) when submitted to none or small horizontal stress (e.g., Borradaile and Jackson, 2010). We sampled different sedimentary facies from very shaly to more calcareous ones where no clear directions of paleocurrent have been observed or characterized at regional scale. The magnetic lineation are always close to the directions of the fold axis (Fig. 6). As a result, we relate the trend of the magnetic lineation to the imprint of deformation, so that the interpreted direction of shortening is NE–SW for sites in the northeast of the Dome and N–S for sites in the southwest. More precisely, the directions slightly change from inner part of the mountain in the northeast (Upper Tinée Valley) to the outer part in the South (southern border of the Dôme of Barrôt) of the area of the Dôme of Barrôt, from N125° to N100°.

In the studied area, the Oligocene and Miocene regional compression directions are believed to be NE–SW and N–S, respectively, deduced from paleostress fault-slip data inversion (Ritz, 1992). NW–SE and E–W trending regional deformation structures, such as major folds and faults, are usually related to the Oligocene or the Miocene compression, respectively. The magnetic lineations present directions compatible with each Oligocene and Miocene main tectonic event. We need to consider the record timing of the magnetic lineation in the cover and in the substratum. However, the fold test (or tilt test) cannot provided a good constraint on the timing of acquisition of AMS shortening directions with respect to tilting (i.e., folding) as described above. Nevertheless, as shown in previous studies in the fold-and-thrust belts elsewhere in the world, the record of "tectonic fabrics" in AMS (i.e., type II or beyond) in weakly deformed sedimentary rocks usually predates folding (Aubourg et al., 2004; Averbuch et al., 1992; Humbert et al., 2012; Kissel et al., 1986; Parés et al., 1999; Weil and Yonkee, 2009). Thus, we propose to attribute the AMS record, all type II–III magnetic fabrics, to the same LPS imprint prior to folding, that is during the beginning of the first compressive event, in the Oligocene time. The deviation of the magnetic lineation in the Permian substratum can be interpreted as the spatial record of the gradual transition from a NE–SW compression in the northeastern side to a N–S compression in the southern. Such deviation of shortening direction has been mentioned in a larger regional scale to be related to the stress deviation in

Table 2
Calculated rotations and inclination differences from the paleomagnetic study. N = number of data used for calculation; D = declination; I = inclination; α_{95} = 95% Fisher confidence error (Fisher, 1953) and corrected Fisher confidence error (Demarest, 1983) for A(+)-group averages; k = dispersion; Rot = rotation along vertical axis, difference in declination with the expected declination for the corresponding virtual magnetic pole of reference; ΔInc = inclination difference, difference in inclination with the expected inclination (positive if reference inclination is higher than observed inclination); Age = age of the virtual magnetic pole of reference for Europe from Torsvik et al. (2008). Averages of both rotation and inclination difference of the set A(+)-group and Mar-A* are calculated as weighted averages.

	N	D (°)	I (°)	α_{95} (°)	k	Rot (°)	ΔInc (°)	Expected magnetization		
								D (°)	I (°)	Age (Ma)
Ser-A	10	310.3	61.9	8.0	37.5	−54.9 ± 10.7	−4.7 ± 5.1			
Rou	13	307.3	67.1	12.5	12	−57.9 ± 21.0	−9.9 ± 8.3			
Leo67-A	16	282.3	50.6	9.4	16.4	−82.9 ± 8.5	+6.6 ± 5.2			
Leo66	5	308.5	50.2	12.6	37.8	−56.8 ± 10.7	+7.0 ± 6.7			
A(+)-group at 75% of unfolding	4	300.9	58.0	9.9	52.1	−64.2 ± 14.4	+0.5 ± 6.0	5.1 ± 3.7	58.5 ± 2.0	25
Mar-B	11	27.0	41.7	10.1	21.3	23.7 ± 7.3	+19.8 ± 5.1	3.4 ± 3.4	61.5 ± 1.6	10
Mar-A*	11	106.0	−62.3	5.9	61.3	−79.7 ± 5.1	−5.2 ± 3.4	5.8 ± 3.5	57.1 ± 1.9	40
A(+)-group and Mar-A*	5	298.2	59.0	7.7	60	−67.4 ± 12.5	−1.7 ± 5.5			

Please cite this article as: Sonnette, L., et al., Significant rotations related to cover–substratum decoupling: Example of the Dôme de Barrôt (Southwestern Alps, France), Tectonophysics (2014), http://dx.doi.org/10.1016/j.tecto.2014.04.009

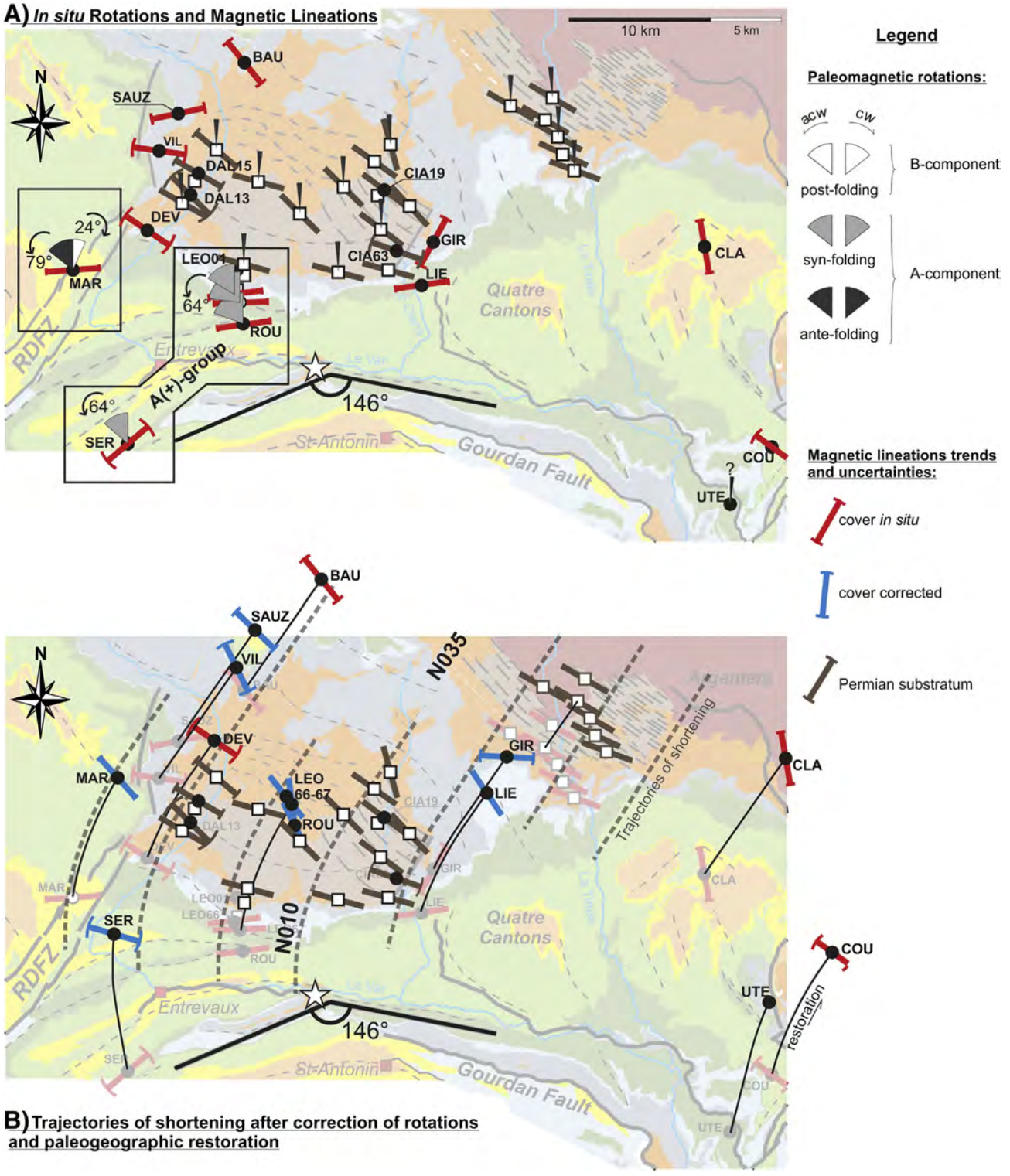

Fig. 6. A) In situ directions of AMS magnetic lineations and horizontal rotations deduced from the paleomagnetic study. B) Magnetic lineations and after correction of the horizontal rotations and 2-D plane restoration of paleogeographic locations before the Oligocene shortening. acw = anticlockwise; cw = clockwise. Only the angular uncertainties of the magnetic lineations determined in these studies are represented. Uncertainties for the magnetic lineations from previous studies are unknown and the uncertainties of the paleomagnetic rotations (see Table 2) are not indicated for clarity of the figure. The trajectories of shortening are inferred from the magnetic lineations of the Permian substratum. The diapir of Puget–Thénier is located by the white star; RDFZ: Rouaine–Daluis Fault Zone. 146° corresponds to the angular difference between the trends of the structures from both sides of the diapir. For the stratigraphy, the tectonic and the sampled sites legends see legend of Fig. 1.

the plate corner due to plate indentation (Huchon et al., 1986; Macedo and Marshak, 1999; Tapponnier and Molnar, 1976), in this case, in the southwestern corner of the French Alps (Collombet et al., 2002 Vialon et al., 1989;). The magnetic lineation of the cover can either be interpreted (1) to mimic the deviation of the magnetic lineation of the Permian substratum, or (2) to be a 30–50° anticlockwise rotation for both the Western and the Southern area. The first interpretation ignores the paleomagnetic rotation of the cover or implies that the rotation predates the AMS record, whereas the second interpretation suggests that the rotation postdates the AMS record.

Please cite this article as: Sonnette, L., et al., Significant rotations related to cover–substratum decoupling: Example of the Dôme de Barrôt (Southwestern Alps, France), Tectonophysics (2014), http://dx.doi.org/10.1016/j.tecto.2014.04.009

5.2. Sources of remagnetization and implication on amount of horizontal block rotation

We found syn-tilting (A-component) and post-tilting (B-component) remagnetizations. Pervasive remagnetization of Mesozoic rocks has been previously reported West of the studied area in similar rock formations in the northern part of the Provence (Katz et al., 2000; Kechra et al., 2003) and in the Digne nappe (Aubourg and Chabert-Pelline, 1999; Cairanne, 2003). The origin of remagnetization is, however, still under debate. Some authors considered that orogenic fluid from Pyrenean orogen might be responsible of pervasive remagnetization (Kechra et al., 2003). Alternatively, some authors proposed that burial might be responsible of the remagnetizations (sedimentary burial for Katz et al., 2000; tectonic burial for Aubourg and Chabert-Pelline, 1999; Cairanne, 2003). Reconciling and favoring the latest hypothesis, we suggest that remagnetization occurred during the tectonic burial resulting from the loading of the Embrunais–Ubaye nappe during the Oligocene (23–34 Ma; Labaume et al., 2008). The onset of schistosity observed at sites VIL, SAUZ and BAU indicates a burial temperature near 250 °C (Chen et al., 2011). In this range of temperature, Aubourg et al. (2012) showed that many magnetic minerals (essentially magnetite) could be neoformed in argillaceous rocks.

The A-components of the A(+)-group highlight the existence of a syn- to post-tilting anticlockwise rotation (Fig. 5C). Assuming that the remagnetization is due to the loading of the Embrunais–Ubaye nappe, the age of remagnetization is estimated at ~25 Ma. The rotational history of the Priabonian blue shale site MAR (Fig. 1B) is more complicated in that it is characterized first by an anticlockwise rotation (MAR-A component), followed by a clockwise rotation (MAR-B component). This complex pattern is potentially related to either the fault activity of the nearby RDFZ or the gravitational sliding in the nappe. However, we cannot make any further interpretation about a regional post-folding clockwise rotation with only one single site; all the rotations related to the site MAR have not been hold for calculation of the average regional rotation. Therefore the paleomagnetic interpretations of the A(+)-group suggest an average of 64 ± 14° syn- or post-folding anticlockwise rotation for sites in the Meso-Cenozoic cover located South of the Dôme de Barrôt and in the fold of Entrevaux (Fig. 6 and Table 2) in accordance with the virtual geomagnetic pole of reference at 25 Ma for Europe (Torsvik et al., 2008). The timing of magnetization thus supports a homogeneous record of the development of magnetic lineation along a NW–SE trend in the cover followed by an anticlockwise rotation.

5.3. Consistency between AMS directions, tectonic structures and the anticlockwise rotation

Our paleomagnetic data show a 64 ± 14° syn- or post-folding anticlockwise rotation of the sedimentary cover for the fold of Entrevaux. A scenario of tectonic structural evolution in terms of LPS direction, highlighted by AMS fabrics (Fig. 3), can be inferred in the Meso-Cenozoic cover. We performed an oroclinal test (Weil and Sussman, 2004; Fig. 7) in which the magnetic lineation has been tested as a proxy for the fold axis. This test is commonly used to decipher the curvature origin of a bent structure. If there is no relation between the trend of the structure and the characterized rotations, that is, the slope of the regression line (Fig. 7) is null and/or the coefficient of determination, R^2, is close to 0, the curvature is considered inherited and is also called a primary arc. This is exactly the case for the magnetic lineation framework of the Permian substratum. If the slope of the regression line equals 1 (Fig. 7), the curvature is due to an oroclinal process (a bend of an orogenic belt imposed after it was formed) and is called an orocline (Carey, 1955) Van der Voo, 2004. If the slope of the regression line is defined between 0 and 1, the curvature is coeval with the formation of the structure and characteristic for a progressive arc. The fold of Entrevaux, according to our 5 surroundings sites of the Meso-Cenozoic cover, would be considered as a progressive arc.

There is also a change in direction of the fold axis from the Southwest to Southeast of the Dome (the center is near the Triassic gypsum diapir of Puget–Théniers) (Figs. 1 and 6). The numbers of folds are greater to the West than to the East of this diapir, which is also correlated with a higher amount of shortening in the western part. Such differential shortening has been analyzed by the study of balanced cross-sections (Laurent et al., 2000). This structural pattern supports the curvature of fold trends with an anticlockwise rotation of around 34° in order to remain parallel the fold of Entrevaux with the layers at North of the Gourdan fault.

The geographical distribution of the LPS directions (Fig. 6A) seems difficult to support the rotations proposed by the paleomagnetic study because the magnetic lineations of the Permian substratum in the southern part of the dome are quite similar to those of the sedimentary cover (ex: sites DEV, LIE, ROU, LEO66 and LEO67). This suggests that the change of the magnetic lineation trends would be the same for both the cover and the substratum, except that the magnetic lineation pattern in the southern part of the cover is affected by an astonishing, 64° anticlockwise rotation. In order to interpret the magnetic lineation patterns in the substratum and the cover, it is necessary to restore the paleogeographic location of the sites before the Miocene event, while the timing of the occurrence of the AMS fabrics. We have to take account into the differential shortening above and below the Triassic décollement surface. Laurent et al. (2000) estimated a 15–20 km southward shortening for the Meso-Cenozoic sedimentary cover and about 7 km of southward shortening for the basement during the Miocene event. Additional shortening of about 4 km is also determined for the Permian substratum between the Dôme de Barrôt and the Upper Tinée Valley (Delteil et al., 2003). Following such results a differential shortening of around 10 km can be estimated between the sedimentary cover surrounding the Dôme de Barrôt and its substratum Permian rocks. However a northward backward restoration does not consider the change in the LPS trends in the Paleozoic substratum and probably overestimate the Miocene event to the detriment of the Oligocene one. Thus, we propose a continuous transition from a thin-skinned tectonics at the Oligocene (i.e., napping via shallow décollement thrusting) to a thick-skinned tectonics during the Miocene (i.e., regional exhumation through a blind deep thrusting). The deviation of the magnetic lineations distribution of the substratum reflects the strain field of the Oligocene event (actually similar to the stress trajectories calculated by Ritz, 1992). In Fig. 6B we backward restored the paleogeographic position of the sampled sites in the sedimentary cover according to the shortening trajectories deduced from the AMS in the substratum. With such type of restoration we also calibrate the original direction of the magnetic lineations from calculated paleomagnetic rotations. As we are not able to determine the paleomagnetic rotations for sites at northwest (VIL, SAUZ and BAU) and east (CLA and COU) of the Dome, we consider two approaches as following.

1. We extrapolated the mean paleomagnetic rotation of the A(+)-group (i.e., syn-tilting event) to the others sites of the sedimentary cover without available rotation data (Fig. 6).
2. We consider the magnetic lineation of the substratum as referenced directions and calculated the corresponding relative rotations (Fig. 8). This approach is inspired from Pueyo Anchuela et al. (2012).

As one can notice in Figs. 6B and 8, the amounts of the paleomagnetic rotations are much larger (about 30°) than those expected from the magnetic lineation pattern of the substratum. That means the advancing motion of the sedimentary cover over the décollement surface according to the deviation of the shortening trends in the Permian substratum, experienced a 30° anticlockwise rotation during it crossed over the Dôme de Barrôt. However, we obtained a maximum of 64° anticlockwise rotation for sites in sedimentary cover. Thus, the other half of about 30°, requires additional rotation(s) through other mechanisms, which certainly need further sampling and analyses of the Meso-Cenozoic cover at North of the dome to be fully explained. We suspect that the magnetic lineation pattern of the cover mimic that of the

Please cite this article as: Sonnette, L., et al., Significant rotations related to cover–substratum decoupling: Example of the Dôme de Barrôt (Southwestern Alps, France), Tectonophysics (2014), http://dx.doi.org/10.1016/j.tecto.2014.04.009

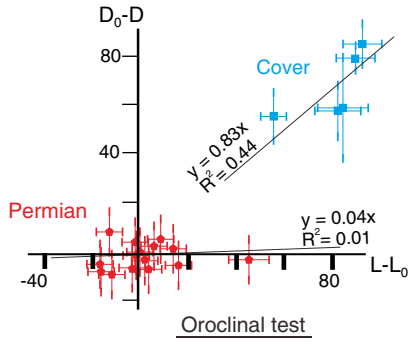

Fig. 7. Oroclinal test (Weil and Sussman, 2004) for Permian and Meso-Cenozoic sites with paleomagnetic declination (D) versus magnetic lineation (L). The reference value for declination is N210° for the substratum and N365° for the cover. The reference value for the magnetic lineation is N120° for the substratum and N000° for the cover.

substratum but with an average direction of N134° (that is the average magnetic lineation trend for sites BAU and COU) rather of N125° (which corresponds to the magnetic lineation trend in the Upper Tine Valley) from the northeastern Dome. This could explain 10° of the total paleomagnetic rotation. Another possibility is to consider that the high décollement efficiency of the gypsum Triassic layer could amplify the rotation initiated by the regional stress deflection pattern. If we referenced to the angular discrepancy between the magnetic lineation of the sites ROU, LEO66 and LEO67 (N085° in average) with that of the sites CIA63 and LEO01 (N105° in average), we could explain the missing 20° of the total paleomagnetic rotation of 64°. In any case, it remains still difficult to fully explain the difference of 64° anticlockwise rotation between the Permian substratum and Meso-Cenozoic cover at the similar geographic positions during the timing of occurrence of AMS fabrics.

5.4. Timing and mechanism responsible for the rotation

Based on the likely important anticlockwise rotation occurred in the South part of the Dome de Barrôt, we propose a tectonic evolution model of double décollement decoupling in the upper crust. The anticlockwise rotation is mechanically accommodated by a cover–substratum decoupling but is also probably affected by right-lateral shearing of the west-bounded RDFZ and/or gravitation sliding after exhumation of the Dome de Barrôt. Concerning the others boundaries, we suppose that the rotation extended at least to the site SAUZ in the northwest, to the site LIE in the east and to the St-Antonin syncline in the south (Fig. 1B).

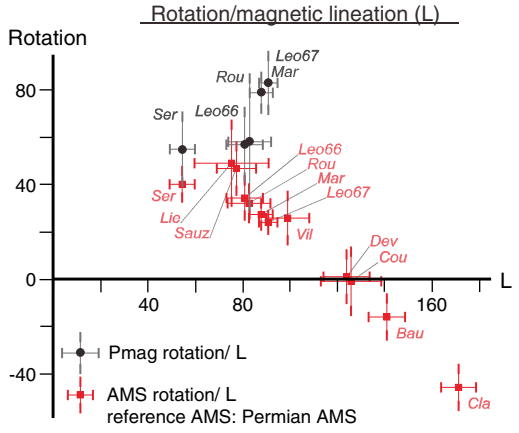

Fig. 8. Diagram of rotation versus magnetic lineation (L). The rotation values of the red squares correspond to the azimuthal difference of the magnetic lineation with the expected magnetic lineation. The rotation values of the black dots correspond to the amount of horizontal rotation determined by the paleomagnetism.

The deposition of the sedimentary cover around the Dôme de Barrôt corresponds to a horst-grabben structure at Liassic time (Dardeau, 1988; Delpech, 1988, Fig. 9A) and was probably a topographic high during Meso-Cenozoic time (Apps et al., 2004); the thickness of the sedimentary cover was about 2–3 km.

In the studied area, two main Tertiary phases of deformation were identified as described below.

1. An Oligocene thin-skinned tectonic event with a tectonic burial of the Dôme de Barrôt at depth around 4–8 km (Siddans, 1980) in response to the overthrusting of the Embrunais–Ubaye nappe (EUN) estimated between 23 and 34 Ma (Labaume et al., 2008, Fig. 9B). During this period, the Meso-Cenozoic sedimentary cover was overlaid by the Embrunais–Ubaye nappe. The increase of the thickness of the Embrunais–Ubaye nappe from 2 to 10 km along a NE trending 50 km long cross-section (Labaume et al., 2008) may imply a slight NW tilting of the underlying cover and substratum, which could explain the geographical extension of the cleavage into the Dôme de Barrôt (Fig. 1A) and the high inclination of the B-components (i.e., post-tilting remagnetization). Such relation if evidenced by further work would constrain significantly both the timing of the folding and the rotation of the cover. The thickness of the Embrunais–Ubaye nappe was greater than or at least similar to that of the underlying Meso-Cenozoic cover in the studied area. The NE–SW trending LPS was presumably recorded during this Oligocene tectonic event. We also proposed during this period the occurrence of a second deeper basal décollement surface developed through the Triassic gypsum layers. It can both explain décollement folding with SW vergence into the cover and the decoupling with the little folded Permian substratum (Fig. 9B).
2. A Miocene thick-skinned tectonics with an exhumation of the Dôme de Barrôt from 23 to 3 Ma, synchronously with the N–S compression (Laurent et al., 2000; Ritz, 1992, Fig. 9C). The most efficient way to accommodate such uplifting is to require crustal deep blind thrusting as proposed by (Ford et al., 1999; Laurent et al., 2000) under the dome. The consequence of the exhumation on the folds of both northern and southern sides of the dome is yet difficult to evaluate, since the vergence of folds is parallel to the expected direction of tilting. The effect of this uplifting was more important on the western and eastern borders where the tilting is oblique to the vergence of the folds. Preliminary field observations in the eastern border of the Dome suggest that the uplifting and possible related gravity sliding seem to have not been much farther extended. It was probably less than 5 km from the Dôme de Barrôt as suggested by the eastward tilting of NW–SE trending compressive structures (which are related to a NE–SW compression) at the eastern border of the Dome. One can also notice that such gravity sliding could explain the orientation of the AMS fabrics of the sites DEV and GIR.

The fold test (McFadden and Jones, 1981) applied on the magnetization of the A(+)-group (Fig. 5C) indicates a maximum value of the dispersion parameter (k) at 75% of unfolding with a declination in the NW quadrant. Such result suggests that an anticlockwise rotation occurred during or after the folding stage and therefore between the late Oligocene to the Pliocene. On such basis, it seems reasonable to correlate this syn-folding magnetization with the peak of the burial event during Oligocene (around 25 Ma) as proposed in Fig. 9B due to the overthrusting and overlying/loading of the Embrunais–Ubaye nappe. As the magnetization was recorded during folding, the anticlockwise rotation of the overlying cover would be coeval with tectonic events from late stage of the Embrunais–Ubaye napping through the tectonic exhumation of the Dôme de Barrôt. Indeed, it is, for a part (~30°) of rotation, can be explained by the regional deflection of the strain shortening trajectories in the Permian substratum (Fig. 6B), which is consistent with a major blind thrust under the Dome. However regarding the regional structures, the Permian substratum of Dôme de Barrôt is bounded by the Oligocene cover on both eastern and western sides: the Oligocene

Please cite this article as: Sonnette, L., et al., Significant rotations related to cover–substratum decoupling: Example of the Dôme de Barrôt (Southwestern Alps, France), Tectonophysics (2014), http://dx.doi.org/10.1016/j.tecto.2014.04.009

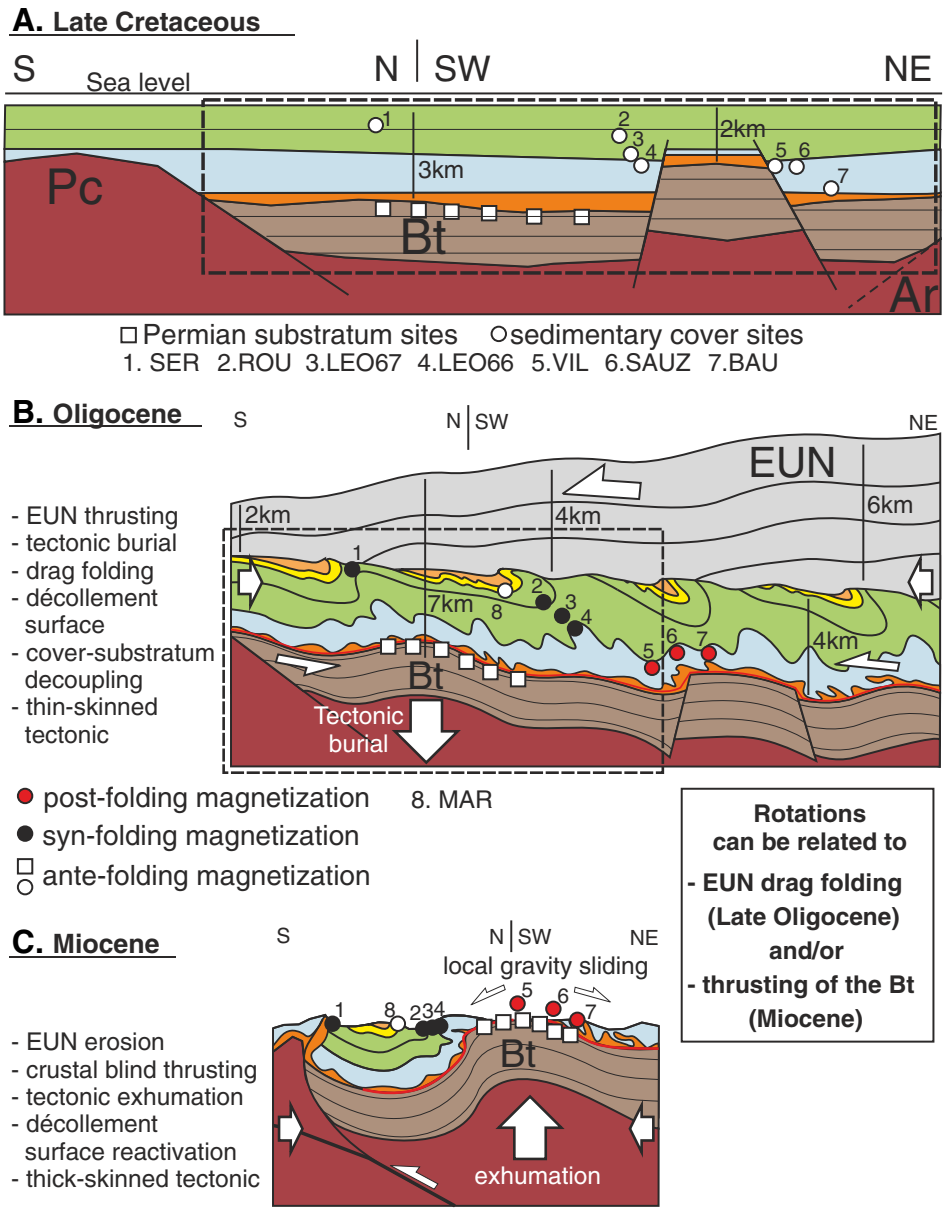

Fig. 9. Synthesis of the geological history of the Dôme de Barrôt in cross-section view. The scale is not respected in the presentation. Same legend as in Fig. 1 and 6. Pc: Provence basement, Bt: Dôme de Barrôt, Ar: Argentera massif, EUN: Embrunnais–Ubaye nappe.

synclines of Grand Coyer in the west and by the syncline of Quatre-Cantons in the east (Figs. 1A and 7). Such structural architecture cannot be explained solely by a uniform crustal blind thrust. It implies a gradually more important exhumation of at least 2 km from E to W (from Quatre-Cantons to the Dôme de Barrôt) and this structure seems to be truncated by the RDFZ on the western side of the Dome, to separate the of Grand Coyer to the west. The southwestward motion of the Digne nappe (over 20 km, Ford et al., 1999, Fig. 1A) was more important than that of the eastern branch of the Castellane salient (about 17 km, ~10 km southward and ~7 km southwestward) according to a thicker sedimentary cover in the northern part of the RDFZ (Macedo and Marshak, 1999). As a result, the fold of Entrevaux in the southern flank of the Dome would be interpreted as a fold drag folded by the sinistral activity of the RDFZ during Mio-Pliocene. Such drag-folding might be responsible for an anticlockwise rotation less than 25°. Whatever the processes evoked to explain the rotation, Embrunais–Ubaye napping and regional deflection of the strain trajectories or RDFZ drag folding and differential motion of the Digne nappe, the gypsum décollement surface acted the major role on accommodating and maybe also amplifying the rotation of the Meso-Cenozoic sedimentary cover. Finally possible local gravitational sliding in the near field around the late exhumed Dôme de Barrôt.

6. Conclusions

The structural and magnetic studies of the Permian substratum Dôme de Barrôt and its surrounding Meso-Cenozoic cover reveal contrasting results:

- The Meso-Cenozoic sedimentary cover in the southern flank of the Dôme de Barrôt, which show an arcuate shape of the stratigraphic and structural trends from SW to SE of the Dome, suggests an anticlockwise rotation along vertical axis of at least 34°, compared to Permian substratum of the Dome itself.
- The magnetic fabrics of the Meso-Cenozoic cover and the Permian substratum both exhibit an arcuate horizontal shortening pattern

Please cite this article as: Sonnette, L., et al., Significant rotations related to cover–substratum decoupling: Example of the Dôme de Barrôt (Southwestern Alps, France), Tectonophysics (2014), http://dx.doi.org/10.1016/j.tecto.2014.04.009

progressively changing from a NE–SW trending in the Northeast to a N–S trending in the South, corresponding to a convex arcuate deviation of stress trajectory.
- Paleomagnetic analysis reveals a 64° anticlockwise rotation at the sites of the cover in the southern flank of the Dôme de Barrôt (i.e., the fold of Entrevaux) whereas the Permian substratum of the Dome recorded no rotation.

When we correct magnetic fabric from paleomagnetic rotation of 64° and by restoring the paleogeographic location of the Meso-Cenozoic cover versus the Paleozoic substratum, there is still an additional 30° anticlockwise rotation that needs to be explained. We propose a tectonic evolution model that a part of the sedimentary cover, the fold of Entrevaux, was detached from the Permian substratum during the overthrusting and advancing of the Embrunnais–Ubaye nappe. It was accompanied by a curved shortening trajectory associated with a 30° anticlockwise rotation in the southern flank of the Dôme de Barrôt. The additional 30° anticlockwise rotation indicated by the paleomagnetic study can be explained by the high decoupling efficiency of the décollement layer and/or the differential motion near the Rouaine–Daluis major transfer fault zone and gravitational sliding in the near field of the Dome. In these scenarios the rotation is mainly accommodated on the sliding of the Triassic gypsum décollement layer, which acted twice. The first décollement allowed cover–substratum decoupling during tectonic burial and folding in Oligocene, and the second once facilitated drag folding and gravity sliding during tectonic exhumation by crustal blind thrusting and sinistral activity of the RDFZ in Miocene.

Acknowledgments

We thank the reviewers (Fabio Speranza and anonymous) and the editor for their comments that helped improving the manuscript. The first author also deeply thanks the Prof. Jacques Angelier who supervised him during his Ph.D thesis and supported him to study the sedimentary cover around the Dôme de Barrôt before passing away in January 2010. This study was part of the Doctorate thesis of the first author at the University of Nice Sophia-Antipolis. We are grateful to Academia Sinica for providing postdoc fellowship to the first author, so that the completion of the manuscript would be possible. This is a contribution of Institute of Earth Science, Academia Sinica (IESAS 1866).

References

Agard, P., Yamato, P., Jolivet, L., Burov, E., 2009. Exhumation of oceanic blueschists and eclogites in subduction zones: timing and mechanisms. Earth Sci. Rev. 92, 53–79.
Apps, G., Peel, F., Elliott, T., 2004. The structural setting and palaeogeographical evolution of the Grès d'Annot Basin. Geol. Soc. Lond., Spec. Publ. 221, 65–96. http://dx.doi.org/10.1144/GSL.SP.2004.221.01.05.
Aubourg, C., Chabert-Pelline, C., 1999. Neogene remagnetization of normal polarity in the Late Jurassic black shales from the southern Subalpine Chains (French Alps). Evidence for late anticlockwise rotations. Tectonophysics 308, 473–486. http://dx.doi.org/10.1016/S0040-1951(99)00145-6.
Aubourg, C., Smith, B., Bakhtari, H., Guya, N., Eshragi, A., Lallemant, S., Molinaro, M., Braud, X., Delaunay, S., 2004. Post-Miocene shortening pictured by magnetic fabric across the Zagros–Makran syntaxis (Iran). Geol. Soc. Am. Spec. Pap. 383, 17–40.
Aubourg, C., Pozzi, J.P., Kars, M., 2012. Burial, claystones remagnetization and some consequences for magnetostratigraphy. Geol. Soc. Lond., Spec. Publ. 371, 181–188.
Averbuch, O., Frizon de Lamotte, D., Kissel, C., 1992. Magnetic fabric as a structural indicator of the deformation path within a fold-thrust structure: a test case from the Corbières (NE Pyrenees, France). J. Struct. Geol. 14, 461–474.
Bogdanoff, S., Schott, J.J., 1977. Etude paléomagnétique et analyse tectonique dans les schistes rouges permiens du Sud de l'Argentera. Bull. Soc. Geol. Fr. 7, 909–916.
Bordet, P., 1950. Le dôme permien de Barrôt (Alpes Maritimes) et son auréole de terrains secondaires. Bull. Serv. Carte Géol. Fr. 43, 1–39.
Borradaile, G.J., 1988. Magnetic susceptibility, petrofabrics and strain. Tectonophysics 156, 1–20.
Borradaile, G., Henry, B., 1997. Tectonic applications of magnetic susceptibility and its anisotropy. Earth Sci. Rev. 42, 49–93.
Borradaile, G.J., Jackson, M., 2010. Structural geology, petrofabrics and magnetic fabrics (AMS, AARM, AIRM). J. Struct. Geol. 32, 1519–1551.
Bourquin, S., Bercovici, A., López-Gómez, J., Diez, J.B., Broutin, J., Ronchi, A., Durand, M., Arché, A., Linol, B., Amour, F., 2011. The Permian–Triassic transition and the onset of Mesozoic sedimentation at the northwestern peri-Tethyan domain scale: palaeogeographic maps and geodynamic implications. Palaeogeogr. Palaeoclimatol. Palaeoecol. 299, 265–280.
Cairanne, G., 2003. Les réaimantations chimiques et le filtrage des polarités du champ magnétique terrestre. Expériences pression–température et comparaison avec des réaimantations naturelles. (Ph.D. thesis) Université de Cergy-Pontoise.
Campredon, R., 1977. Les formations paléogènes des Alpes Maritimes franco–italiennes. (Ph.D. thesis) Université de Nice.
Campredon, R., Bordet, P., Giannerini, G., Manigault, B., 1980. Carte géologique de la France au 1/50000, feuille Entrevaux, BRGM Editions, Orléans.
Carey, S.W., 1955. The orocline concept in geotectonics—Part I. Papers and proceedings of the Royal Society of Tasmania, pp. 255–288.
Chen, C.T., Chan, Y.C., Lu, C.Y., Simoes, M., Beyssac, O., 2011. Nappe structure revealed by thermal constraints in the Taiwan metamorphic belt. Terra Nova 23, 85–91.
Cogné, J.P., 2003. Paleomac: a macintosh™ application for treating paleomagnetic data and making plate reconstructions. Geochem. Geophys. Geosyst. 4, 1–8. http://dx.doi.org/10.1029/2001GC000227.
Cogné, J.P., Perroud, H., 1985. Strain removal applied to paleomagnetic directions in an orogenic belt: the Permian red slates of the Alpes Maritimes, France. Earth Planet. Sci. Lett. 72, 125–140.
Collombet, M., Thomas, J.C., Chauvin, A., Tricart, P., Bouillin, J.P., Gratier, J.P., 2002. Counterclockwise rotation of the Western Alps since the Oligocene: new insights from paleomagnetic data. Tectonics 21. http://dx.doi.org/10.1029/2001TC901016 (14-1–14-15).
Costa, E., Vendeville, B., 2002. Experimental insights on the geometry and kinematics of fold-and-thrust belts above weak, viscous evaporitic décollement. J. Struct. Geol. 24, 1729–1739. http://dx.doi.org/10.1016/S0191-8141(01)00169-9.
Cotillon, P., 1971. Le Crétacé inférieur de l'Arc subalpin de Castellane entre l'Asse et le Var, stratigraphie et sédimentologie. Mémoires du B.R.G.M., Orléans, 68, pp. 1–313.
Dahlen, F., Suppe, J., Davis, D., 1984. Mechanics of fold-and-thrust belts and accretionary wedges: cohesive Coulomb theory. J. Geophys. Res. Solid Earth 89, 10087–10101 (1978–2012).
Dardeau, G., 1988. Tethyan evolution and alpine reactivation of Jurassic extensional structures in the French "Alpes Maritimes". Bull. Soc. Geol. Fr. IV, 651–657. http://dx.doi.org/10.2113/gssgfbull.IV.4.651.
De Graciansky, P.C., Lemoine, M., 1988. Early cretaceous extensional tectonics in the southwestern French Alps: a consequence of North-Atlantic rifting during Tethyan spreading. Bull. Soc. Geol. Fr. 8, 733–737.
Delpech, P.Y., 1988. Rifting Jurassique sur la bordure occidentale du dôme de Barrôt (Alpes occidentales françaises). Evolution géodynamique d'un secteur de la Marge nord-téthysienne. (Ph.D. thesis) Université de Pierre et Marie Curie, Paris.
Delteil, J., Stéphan, J.F., Attal, M., 2003. Control of Permian and Triassic faults on alpine basement deformation in the Argentera massif (external Southern French Alps). Bull. Soc. Geol. Fr. 174, 481–496. http://dx.doi.org/10.2113/174.5.481.
Demarest, H.H., 1983. Error analysis for the determination of tectonic rotation from paleomagnetic data. J. Geophys. Res. Solid Earth 88, 4321–4328. http://dx.doi.org/10.1029/JB088iB05p04321.
Fisher, R., 1953. Dispersion on a sphere. Proc. R. Soc. Lond. Ser. A Math. Phys. Sci. 217, 295–305.
Ford, M., Lickorish, W., Kusznir, N., 1999. Tertiary foreland sedimentation in the southern subalpine chains, SE France: a geodynamic appraisal. Basin Res. 11, 315–336.
Giannerini, G., Sanchez, G., Schreiber, D., Lardeaux, J.M., Rolland, Y., de Castro, A.B., Bauve, V., 2011. Geometry and sedimentary evolution of the transpresssive Roquebrune–Cap Martin basin: implications on the kinematics and timing of the Nice arc deformation during Miocene times, SW Alps. Bull. Soc. Geol. Fr. 182, 493–506.
Goguel, J., Faure-Muret, A., Fallot, P., Bordet, P., Lemoine, M., 1957. Carte géologique de la France au 1/50000, feuille Puget–Théniers, BRGM Editions, Orléans.
Graham, R., 1978. Quantitative deformation studies in the Permian rocks of the Alpes-Maritimes. Proceedings Symposium in Honour of Prof. J. Goguel, BRGM. BRGM, Ed., Orléans, pp. 219–238.
Graham, R., 1981. Gravity sliding in the Maritime Alps. Geol. Soc. Lond., Spec. Publ. 9, 335–352.
Gubler, Y., Héritier, F., Schlund, J.M., Verrier, G., Chavand, J.C., Kerckhove, C., Goguel, J., 1967. Carte géologique de la France au 1/50000, feuille Allos, BRGM Editions.
Henry, B., 1973. Studies of microtectonics, anisotropy of magnetic susceptibility and paleomagnetism of the Permian Dôme de Barrôt (France): paleotectonic and paleosedimentological implications. Tectonophysics 17, 61–72. http://dx.doi.org/10.1016/0040-1951(73)90065-6.
Huchon, P., Barrier, E., de Bremaecker, J.C., Angelier, J., 1986. Collision and stress trajectories in Taiwan: a finite element model. Tectonophysics 125, 179–191. http://dx.doi.org/10.1016/0040-1951(86)90013-2.
Humbert, F., Robion, P., Louis, L., Bartier, D., Ledésert, B., Song, S.R., 2012. Magnetic inference of in situ open microcracks in sandstone samples from the Taiwan Chelungpu fault drilling project (TCDP). J. Asian Earth Sci. 45, 179–189.
Jelínek, V., 1978. Statistical processing of anisotropy of magnetic susceptibility measured on groups of specimens. Stud. Geophys. Geod. 22, 50–62.
Jelinek, V., 1981. Characterization of the magnetic fabric of rocks. Tectonophysics 79, T63–T67.
Katz, B., Elmore, R.D., Cogoini, M., Engel, M.H., Ferry, S., 2000. Associations between burial diagenesis of smectite, chemical remagnetization, and magnetite authigenesis in the Vocontian trough, SE France. J. Geophys. Res. Solid Earth 105, 851–868 (1978–2012).
Kechra, F., Vandamme, D., Rochette, P., 2003. Tertiary remagnetization of normal polarity in Mesozoic marly limestones from SE France. Tectonophysics 362, 219–238. http://dx.doi.org/10.1016/S0040-1951(02)00639-X.
Kissel, C., Barrier, E., Laj, C., Lee, T.Q., 1986. Magnetic fabric in undeformed marine clays from compressional zones. Tectonics 5, 769–781.

Please cite this article as: Sonnette, L., et al., Significant rotations related to cover–substratum decoupling: Example of the Dôme de Barrôt (Southwestern Alps, France), Tectonophysics (2014), http://dx.doi.org/10.1016/j.tecto.2014.04.009

Kligfield, R., Owens, W., Lowrie, W., 1981. Magnetic susceptibility anisotropy, strain, and progressive deformation in Permian sediments from the Maritime Alps (France). Earth Planet. Sci. Lett. 55, 181–189.
Kruiver, P.P., Dekkers, M.J., Langereis, C.G., 2000. Secular variation in Permian red beds from Dôme de Barrôt, SE France. Earth Planet. Sci. Lett. 179, 205–217.
Labaume, P., Jolivet, M., Souquière, F., Chauvet, A., 2008. Tectonic control on diagenesis in a foreland basin: combined petrologic and thermochronologic approaches in the Grès d'Annot basin (late Eocene–early Oligocene, French–Italian external Alps). Terra Nova 20, 95–101.
Laurent, O., Stéphan, J.F., Popoff, M., 2000. Modalités de la structuration miocène de la branche sud de l'arc de Castellane (chanes subalpines méridionales). Géol. Fr. 3, 33–65.
Lowrie, W., 1990. Identification of ferromagnetic minerals in a rock by coercivity and unblocking temperature properties. Geophys. Res. Lett. 17, 159–162.
Macedo, J., Marshak, S., 1999. Controls on the geometry of fold–thrust belt salients. Geol. Soc. Am. Bull. 111, 1808–1822.
Malavieille, J., 2010. Impact of erosion, sedimentation, and structural heritage on the structure and kinematics of orogenic wedges: analog models and case studies. GSA Today 20, 4–10.
McFadden, P., Jones, D., 1981. The fold test in paleomagnetism. Geophys. J. R. Astron. Soc. 67, 53–58.
Parés, J.M., 2004. How deformed are weakly deformed mudrocks? Insights from magnetic anisotropy. Geol. Soc. Lond., Spec. Publ. 238, 191–203.
Parés, J.M., van der Pluijm, B.A., Dinarès-Turell, J., 1999. Evolution of magnetic fabrics during incipient deformation of mudrocks (Pyrenees, northern Spain). Tectonophysics 307, 1–14. http://dx.doi.org/10.1016/S0040-1951(99)00115-8.
Pueyo Anchuela, Ó., Pueyo, E., Pocoví Juan, A., Gil Imaz, A., 2012. Vertical axis rotations in fold and thrust belts: comparison of AMS and paleomagnetic data in the western external Sierras (southern Pyrenees). Tectonophysics 532, 119–133.
Ritz, J.F., 1992. Tectonique récente et sismotectonique des Alpes du Sud: analyses en termes de contraintes. Quaternaire 3, 111–124.
Robion, P., Grelaud, S., Frizon de Lamotte, D., 2007. Pre-folding magnetic fabrics in fold-and-thrust belts: why the apparent internal deformation of the sedimentary rocks from the Minervois basin (NE Pyrenees, France) is so high compared to the Potwar basin (SW Himalaya, Pakistan)? Sediment. Geol. 196, 181–200.
Sanchez, G., Rolland, Y., Jolivet, M., Brichau, S., Corsini, M., Carter, A., 2011a. Exhumation controlled by transcurrent tectonics: the Argentera–Mercantour massif (SW Alps). Terra Nova 23, 116–126.
Sanchez, G., Rolland, Y., Schneider, J., Corsini, M., Oliot, E., Goncalves, P., Verati, C., Lardeaux, J.M., Marquer, D., 2011b. Dating low-temperature deformation by $^{40}Ar/^{39}Ar$ on white mica, insights from the Argentera–Mercantour massif (SW Alps). Lithos 125, 521–536.
Schuiling, R., 1956. Jointing in the Permian Dôme de Barrôt. Neth. J. Geosci./Geol. Mijnb. 18, 227–234.
Siddans, A., 1979. Arcuate fold and thrust patterns in the subalpine chains of southeast France. J. Struct. Geol. 1, 117–126.
Siddans, A., 1980. Compaction, métamorphisme et structurologie des argilites permiennes dans les Alpes-Maritimes (France). Rev. Géol. Dynam. Géog. Phys. 22, 279–292.
Siddans, A., Henry, B., Kligfield, R., Lowrie, W., Hirt, A., Percevault, M., 1984. Finite strain patterns and their significance in Permian rocks of the Alpes Maritimes (France). J. Struct. Geol. 6, 339–368.
Sztrákos, K., du Fornel, É., 2003. Stratigraghy, paleoecology and foraminifers of the paleogene from the Alpes de Haute-Provence and the Alpes Maritimes. Rev. Micropaleontol. 46, 229–267.
Tapponnier, P., Molnar, P., 1976. Slip-line field theory and large-scale continental tectonics. Nature 264, 319–324.
Torsvik, T.H., Müller, R.D., Van der Voo, R., Steinberger, B., Gaina, C., 2008. Global plate motion frames: toward a unified model. Rev. Geophys. 46, 44p. http://dx.doi.org/10.1029/2007RG000227.
Van den Ende, C., 1977. Palaeomagnetism of Permian Red Beds of the Dôme de Barrôt (S. France). (Ph.D. thesis) Rijks-universiteit Utrecht.
Van der Voo, R., 2004. Paleomagnetism, oroclines, and growth of the continental crust. GSA Today 14, 4–9. http://dx.doi.org/10.1130/1052-5173(2004)014<4:POAGOT>2.0.CO;2.
Vernet, J., 1958. Sur la tectonique du socle permo-werfenien du Dôme de Barrôt. 34. Travaux du laboratoire de Géologie de la Faculté des Sciences de l'Université de Grenoble pp. 219–290.
Vialon, P., Rochette, P., Ménard, G., 1989. Indentation and rotation in the Western Alpine Arc. Geol. Soc. Lond., Spec. Publ. 45, 329–338. http://dx.doi.org/10.1144/GSL.SP.1989.045.01.18.
Vidal-Royo, O., Koyi, H.A., Muñoz, J.A., 2009. Formation of orogen-perpendicular thrusts due to mechanical contrasts in the basal décollement in the central external Sierras (southern Pyrenees, Spain). J. Struct. Geol. 31, 523–539.
Weil, A.B., Sussman, A.J., 2004. Classifying curved orogens based on timing relationships between structural development and vertical-axis rotations. Orogenic Curvature: Integrating Paleomagnetic and Structural Analyses, 383 pp. 1–16.
Weil, A.B., Yonkee, A., 2009. Anisotropy of magnetic susceptibility in weakly deformed red beds from the Wyoming salient, Sevier thrust belt: relations to layer-parallel shortening and orogenic curvature. Lithosphere 1, 235–256.
Westphal, M., 1976. Contribution du paléomagnétisme à l'étude des déplacements continentaux autour de la Méditerranée occidentale. (Ph.D. thesis) Université de Strasbourg.
Zjiderveld, J.D.A., 1975. Paleomagnetism of the Esterel Rocks. (Ph.D. thesis) University of Utrecht.

Please cite this article as: Sonnette, L., et al., Significant rotations related to cover–substratum decoupling: Example of the Dôme de Barrôt (Southwestern Alps, France), Tectonophysics (2014), http://dx.doi.org/10.1016/j.tecto.2014.04.009